*Published online 26 December 2013*

*Nucleic Acids Research, 2014, Vol. 42, No. 6* ***e40***
*doi:10.1093/nar/gkt1287*

# Redirecting splicing with bifunctional oligonucleotides

**Jean-Philippe Brosseau[1,2], Jean-François Lucier[1,3], Andrée-Anne Lamarche[3], Lulzim Shkreta[3], Daniel Gendron[1], Elvy Lapointe[1], Philippe Thibault[1], Éric Paquet[1], Jean-Pierre Perreault[1,2], Sherif Abou Elela[1,3] and Benoit Chabot[1,3,*]**

[1]Laboratory of Functional Genomics and Research Centre on RNA Biology of the Université de Sherbrooke, Sherbrooke, Quebec J1E 4K8, Canada, [2]Department of Biochemistry, Faculty of Medicine and Health Sciences, Université de Sherbrooke, Sherbrooke, Quebec J1E 4K8, Canada and [3]Department of Microbiology and Infectious Diseases, Faculty of Medicine and Health Sciences, Université de Sherbrooke, Sherbrooke, Quebec J1E 4K8, Canada

Received July 8, 2013; Revised October 21, 2013; Accepted November 18, 2013

## ABSTRACT

**Ectopic modulators of alternative splicing are important tools to study the function of splice variants and for correcting mis-splicing events that cause human diseases. Such modulators can be bifunctional oligonucleotides made of an antisense portion that determines target specificity, and a non-hybridizing tail that recruits proteins or RNA/protein complexes that affect splice site selection (TOSS and TOES, respectively, for targeted oligonucleotide silencer of splicing and targeted oligonucleotide enhancer of splicing). The use of TOSS and TOES has been restricted to a handful of targets. To generalize the applicability and demonstrate the robustness of TOSS, we have tested this approach on more than 50 alternative splicing events. Moreover, we have developed an algorithm that can design active TOSS with a success rate of 80%. To produce bifunctional oligonucleotides capable of stimulating splicing, we built on the observation that binding sites for TDP-43 can stimulate splicing and improve U1 snRNP binding when inserted downstream from 5′ splice sites. A TOES designed to recruit TDP-43 improved exon 7 inclusion in *SMN2*. Overall, our study shows that bifunctional oligonucleotides can redirect splicing on a variety of genes, justifying their inclusion in the molecular arsenal that aims to alter the production of splice variants.**

## INTRODUCTION

Alternative splicing is the process by which exons are differentially combined to produce different types of mRNAs from a single gene. This process allows cells to produce an average of 8–10 splice variants per gene, substantially increasing the coding capacity of the human genome (1–3) and making an immense contribution to the structural and functional diversity of our proteome (4). Defects in alternative splicing contribute to many human diseases including spinal muscular atrophy (SMA), myotonic dystrophy and cancer (5,6). In addition, it is estimated that as many as 60% of human diseases might be caused by point mutations that alter splicing (e.g. β-thalassemia, cystic fibrosis and progeria) (7), However, the function of the majority of splicing isoforms and the real number of human diseases affected by splicing remain unclear.

Molecular tools that can specifically alter the proportion of splice variants are essential to assess the function of a multitude of splice variants. Unfortunately, deducing the function of splice variants by RNA interference approaches is challenging because decreasing the level of a given splice variant also changes the total amount of products for that gene (8). Therefore, alternative approaches are needed to alter the production of splice variants by redirecting splicing decisions without changing the overall level of gene expression. The original strategy, pioneered by the group of Kole, used an antisense oligonucleotide (ASO) complementary to a cryptic splice site in the β-globin gene that prevented its use and favored selection of the authentic site (9). This approach has since been used regularly to alter the proportion of splice variants produced from mutated genes or alternative splicing units [(10), reviewed in (11,12)]. Since a shift in splicing does not in principle alter the absolute amount of gene products, this approach increases the confidence of attributing a function to a specific splice variant.

Given that alternative splicing decisions are often controlled by regulatory proteins bound to exonic and

*To whom correspondence should be addressed. Tel: +819 820 6868 (ext. 75321); Fax: +819 820 6831; Email: benoit.chabot@usherbrooke.ca

intronic elements located in the vicinity of alternative splice sites, the ASO approach has evolved to target these elements and prevent them from recruiting regulatory proteins (13–15). This new strategy was used successfully to abrogate the action of an intronic splicing silencer within the *SMN2* gene, increase exon 7 inclusion and improve the SMA-associated cellular phenotype (16–18). Splice switching oligonucleotides in the same design category are being tested for other diseases [reviewed in (12,19)], including Duchenne muscular dystrophy (20–22).

Another splice switching strategy is to use oligonucleotides that contain a portion complementary to the target site linked to a non-hybridizing tail that can provide either stimulatory or repressor function. When the tail contains binding sites for hnRNP A1, positioning such an oligonucleotide upstream of a 5′ splice site (5′ss) interferes with U1 snRNP binding and repress splice site use (23). This bifunctional oligonucleotide design has been coined TOSS for targeted oligonucleotide silencer of splicing (11). Although the inhibitory potential of tails bound by other proteins has not been examined systematically, exon-binding oligonucleotides with tails carrying splicing signals also displayed strong inhibitory activity (23,24). TOSS with A1 tails have been used successfully to repress exon 8 in *SMN2*, hence redirecting splicing to favor exon 7 inclusion in the fibroblasts of SMA patient and in a mouse model of SMA (25). In contrast, bifunctional A1 binding oligonucleotides positioned in introns can stimulate splicing of long introns *in vivo* and can elicit skipping of an intervening 5′ss in splicing extracts (26).

Bifunctional oligonucleotides carrying a tail designed to stimulate splice site usage are coined TOES for targeted oligonucleotide enhancer of splicing (27). This category includes oligonucleotides that contain a tail that recruits positively acting SR proteins (28) or a tail made of a synthetic RS domain covalently linked to an antisense moiety (29). A splicing enhancer element was also engineered in the U7 snRNA sequence which when expressed in SMA cells stably stimulated *SMN2* exon 7 inclusion (30).

To assess the biological function of a growing repertoire of splice variants, we need approaches that can change the relative abundance of such variants. Although bifunctional oligonucleotides are in principle ideally suited to assess isoform function, their use has remained restricted to only a handful of cases. To validate the broad applicability of bifunctional oligonucleotides, we show that TOSS can repress splice site use on a wide spectrum of targets, leading to an algorithm that can design active TOSS with a success rate of 80%. As for the alternative strategy that aims to stimulate splice site utilization, we describe a new TOES design that uses a TDP-43 binding tail to promote exon inclusion. Our results validate the use of bifunctional oligonucleotides to alter splicing decisions on an expanding repertoire of targets, and make them attractive as individual or high-throughput tools to modulate the production of splice variants.

## MATERIALS AND METHODS

### Cell culture and transfection

SKOV3ip1, NIH-OVCAR-3, PC-3, ZR-75-1 and OVC-116 cell lines have been described previously (31). TOSS and ASO were synthesized as 2′OMe and standardly desalted by IDT (USA). Oligonucleotides purity was assessed by fractionation on 15% denaturing acrylamide gels. Oligonucleotides were diluted in Opti-MEM to which an equivalent volume of Lipofectamine 2000 was added. The mixture was added to cells that had been previously seeded in a 6- or 96-well plate with complete media. The final concentration of oligonucleotide was 150 nM for TOES and 400 nM for TOSS and ASO. TOSS and ASO were transfected in biological triplicates (three transfections using different cell passages).

### RNA extraction and RT-PCR

RNA was extracted 24 h post-transfection using either Trizol (Invitrogen) or a silica-based column (Absolutely RNA 96 Microprep kit from Stratagene) (32). We followed the manufacturer's instruction for Trizol (Invitrogen) extraction except that linear acrylamide (5 μg) was added during isopropanol precipitation. Integrity and quality of RNA was evaluated by Agilent Bioanalyzer and Nanodrop, respectively. The level of contaminating genomic DNA was examined as described elsewhere (33). The TOSS-induced splicing shift was evaluated by endpoint RT-PCR and quantitative RT-PCR. The design of endpoint RT-PCR primers was performed as described previously (33). The endpoint PCR assays were performed using the Qiagen One step RT-PCR kit (Qiagen) using the gene-specific reverse primer in the reverse transcription step. PCR products were fractionated on a Caliper 90 workstation as described previously (33). The percent of splicing index (Psi or ψ value) were calculated for each sample, and the $\Delta\psi$ ($\psi_{LF} - \psi_{TOSS}$) was used to monitor the efficiency of TOSS-induced splicing shift. Design and validation of quantitative RT-PCR assays were done as previously described (32,34). For each alternative splicing events followed by endpoint RT-PCR, a long-specific, a short-specific and a global (targeting all isoforms) primer pairs were designed whenever possible. Following a random priming strategy (random hexamers) and quantitative RT-PCR fluorescence measurement using SYBR Green, two analytical strategies were used. One is the relative expression normalized by housekeeping as previously described (32). The second is the quantitative splicing index, which corresponds to the percentage of the longer isoform over the sum of the short and long isoforms (32).

### Western analysis

Proteins were separated by SDS–PAGE and transferred onto nitrocellulose Hybond C (Amersham) using a transfer buffer (1.45% glycine, 0.3% Tris-base and 25% methanol) for 6 h at 70 V and 4°C. The membrane was washed with TBS (0.24% Tris–HCl, 0.8% NaCl, pH 8.0) for 5 min and then incubated for 1.5 h at 4°C with TBST (TBS + 0.05% Tween 20 and 5% milk powder).

After blocking, the membrane was incubated with the antibody at room temperature for 2 h. The membrane was washed twice with TBST, and the secondary antibody was added and incubated for 1 h. Detection was performed with ECL (Amersham Biosciences) according to the manufacturer's recommendations.

### In vitro splicing assay and oligonucleotide-mediated RNase H protection assay

Splicing assays were performed as described (35) using HeLa nuclear extracts (36). RNase H protection assay was performed as follows: to 4 µl of HeLa extract are added 0.5 µl of rATP 12.5 mM, 0.5 µl of $MgCl_2$ 80 mM, 0.5 µl of creatine phosphate 0.5 M, 2.5 µl of PVA 13%, 0.25 µl of DTT 0.1 M, 0.25 µl of RNAguard 40 U/µl, 0.25 µl of KCl 1 M, 1.375 µl of buffer D (35) and 0.25 µl of RNase H 5 units/µl. One microliter of radiolabeled RNA is added (30 000 cpm) and 1 µl of creatine kinase (1 U/µl). Mixtures were incubated 0, 5 or 20 min at 30°C and then placed on ice. In total, 0.75 pmol of oligonucleotides 7A-A5 and 7B-A5 (35) are added with 2.5 U of RNase H, and incubation is carried out for 15 min at 30°C. RNA is then phenol extracted after adding 500 µl of extraction buffer (0.3 M sodium acetate, 0.2% of SDS), and ethanol precipitated. RNA is resuspended in formamide dyes, boiled, loaded and fractionated on a denaturing acrylamide gel.

### Construction of the inducible shTDP/HeLa cell line

Oligonucleotides corresponding to TDP-43 were shTDP-43Bfwd 5′-GATCCCACTACAATTGATATCAAATTCAAGAGATTTGATATCAATTGTAGTGTTTTTGGAAA-3′ and shTDP-43Brev 5′-AGCTTTTCCAAAAACACTACAATTGATATCAAATCTCTTGAATTTGATATCAATTGTAGTGGG-3′. After duplex formation, they were inserted at the BglII and HindIII sites in plasmid pTER + which was transfected in HeLa cells already expressing the transcriptional repressor (via expression of plasmid pCDNA 6/TR). Four hours post-transfection, DMEM with 400 µg/ml of zeocine and 3 µg/ml of blasticidine was added to select for the presence of both plasmids. Distinct clones were isolated and induced with 1.5 µg/ml of doxycycline to test for the depletion of TDP-43.

## RESULTS

### Measuring TOSS efficacy

We have shown previously that a bifunctional interfering oligonucleotide (TOSS A1_Bclx4) containing a 2′OMe tail with hnRNP A1 binding sites and a sequence complementary to the −4 to −24 region upstream of the Bcl-xL 5′ss region can shift *Bcl-x* splicing from the long variant (Bcl-xL) to the short variant (Bcl-xS) in human PC-3 and HCT-116 cells (23) (Figure 1A and B). Quantitative RT-PCR indicates that the shift in the production of *Bcl-x* variants is caused by a reduction in Bcl-xL and an increase in Bcl-xS (Figure 1C), suggesting that the repressive effect of the TOSS on the 5′ss of Bcl-xL improves the competitivity of the 5′ss of Bcl-xS. However, it is difficult to exclude the possibility that the observed effect was at least in part due to the interference of the TOSS with the reverse transcription step required for PCR analysis (Supplementary Figure S1a). To evaluate this possibility, we measured the effects of adding TOSS to total RNA prior to reverse transcription and PCR amplification. Increasing amounts of TOSS targeting three different genes (*Bcl-x*, *APAF1* and *CAPN3*) were added immediately before the reverse transcription step and the splicing pattern determined using PCR. In all cases, the synthesis of the longer product was inhibited, even at concentrations as low as 4 nM (Supplementary Figure S1b). This result suggests that the TOSS remaining in the total RNA samples extracted from transfected cells may alter the splicing isoform ratio and lead to an overestimation of TOSS efficiency. The impact of TOSS on the splicing pattern estimated by PCR varied based on the procedure used for RNA extraction. Column-based purification procedure did not fully remove the TOSS in RNA samples (37), while Trizol-based extraction removed the oligonucleotide from the aqueous phase (Supplementary Figure S2) and eliminated the artifactual impact of TOSS during RT-PCR (Supplementary Figure S3). However, while Trizol extraction eliminates the RT-PCR artifact, this step is inconvenient when multiple samples must be analyzed in a high-throughput manner. Since none of the commercially available high-throughput RNA purification kits tested removed TOSS from the RNA samples, modifications of the RNA extraction procedure do not provide a practical approach for the elimination of TOSS interference when detecting alternative splicing using RT-PCR.

To obtain an unbiased estimate of the *in vivo* impact of TOSS on the production of splice isoforms, we performed quantitative RT-PCR to detect the short and long variants individually. While the long variant values could vary depending on the method of RNA purification, the values for the short variant were similar, as expected because these variants lack sequences complementary to the TOSS (Supplementary Figure S4). Measuring the short variant by quantitative RT-PCR, therefore, accurately assess the shift in splicing regardless of the presence of TOSS in the reverse transcription reaction. We conclude that if Trizol extraction cannot be accommodated, the reliable monitoring of the effects of bifunctional oligonucleotides requires PCR methods that exclude the amplification of the targeted sequence.

To further confirm the PCR estimates of the TOSS-dependent splicing shift we analyzed the ratio of the protein isoforms after exposure to TOSS and compared it to the PCR pattern. As shown in Figure 1D, the western blot of CASP8 and CASP10 isoforms, which are used as model genes, were altered in the same direction and produced a splicing ratio similar to that detected by PCR using the same samples (37).

### Structural elements affecting TOSS efficacy

With the goal of improving the design of TOSS, we evaluated some of the parameters that affect TOSS activity. To control intra- and intermolecular secondary

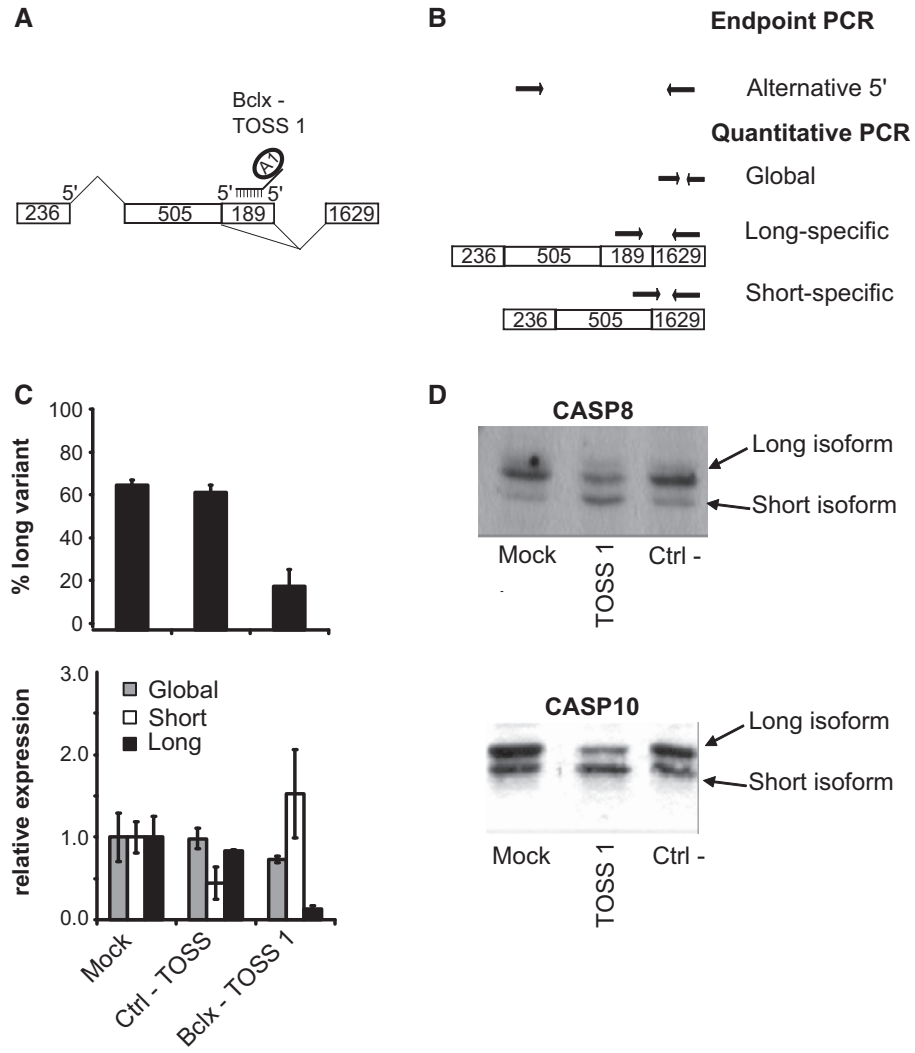


**Figure 1.** Impact of TOSS on the production of apoptotic splice variants. **(A)** Schematic representation of the *Bcl-x* splicing unit and the location of Bclx–TOSS1. **(B)** Positions of the PCR primers used to quantify splice variants of *Bcl-x*. **(C)** Histograms representing average percentage values obtained by endpoint RT-PCR (upper panel) or the relative expression of variants by quantitative RT-PCR (bottom panel) in three biological replicates. PC-3 cells were transfected with Bclx–TOSS1 (400 nM final concentration) or a control TOSS carrying an antisense sequence not complementary to *Bcl-x* (ctrl–TOSS). Total RNA was extracted with Trizol 24 h later. **(D)** Western analysis of TOSS-induced shifts in CASP protein isoforms. HeLa cells were transfected with CASP8–TOSS1 and a mutated version (ctrl–TOSS) containing four mismatches (upper panel) or CASP10–TOSS1 and a mutated version (ctrl–TOSS) containing two mismatches (bottom panel). Proteins were extracted 72 h later, and the proportion of the splice variants was verified by western analysis.

structures that could interfere with the interaction of TOSS with its target RNA we use the UNAFold software package (38) to predict the minimal $\Delta G$ of TOSS. By examining the impact of previously tested TOSS with different $\Delta G$, we found that a $\Delta G$ superior to $-9.4$ kcal/mol, which is two standard deviations away from the average free energy of a thousand randomly designed TOSS, generally yielded TOSS with efficient and reproducible modulation of alternative splicing. Other parameters were taken into account such as GC content, polynucleotide repeats and innate immune response activating sequences (Figure 2).

We also evaluated the general requirement of the tail of TOSS because although it was previously shown that a tail that binds hnRNP A1 was required for maximal modulation of *Bcl-x* splicing, it was not clear if this was true for other target genes (23). Therefore, we generated ASOs containing (TOSS) or lacking a tail (ASO) against 10 different splicing events and monitored their impact on splicing. A splicing shift was acknowledged when either the short or long splice variant changed by at least 2-fold. As shown in Figure 3, eight ASOs modulated splicing without affecting the overall level of gene expression, while the ASO targeting *SYK* affected both splicing and global gene expression. On the other hand, seven of the eight TOSS that modulated alternative splicing did so in a manner superior to the corresponding ASO (Figure 3). We also noted a large increase in short isoforms when TOSS were targeting *CCNE1*, *KITG*, *LIG4* and *MCL1*, ruling out any over estimation of the splicing shift by the interfering RT-PCR artifact. Even if residual amounts were present, we observed that ASO

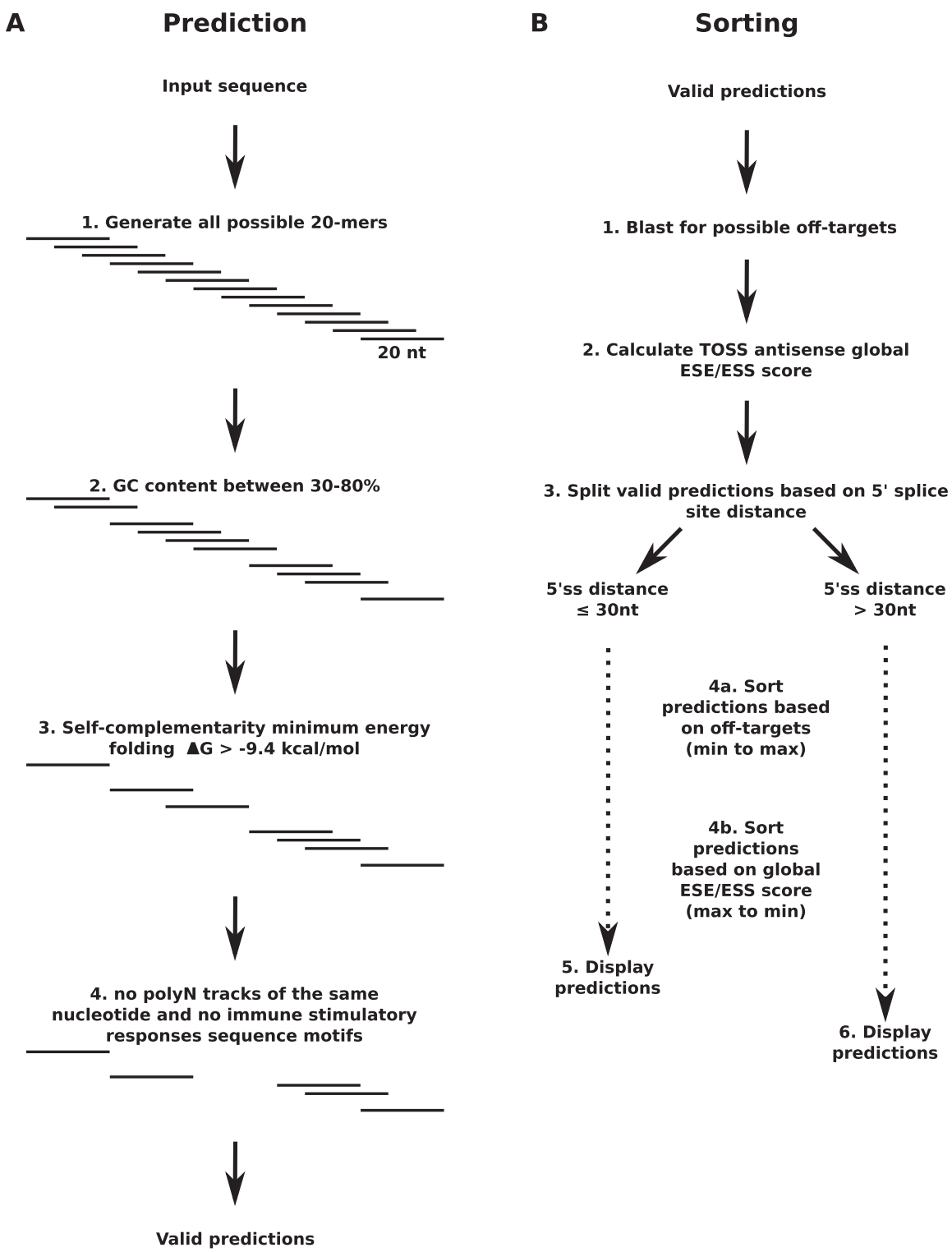


**Figure 2.** Development of the algorithm for designing TOSS. An application programming interface (API) and web application was developed using Perl version 5.8.8 (the Perl directory http://www.perl.org/) with CGI::Application, HTML::Template and Bioperl CPAN modules (CPAN: Comprehensive Perl Archive Network, http://cpan.org/). **(A)** To perform TOSS prediction, the user specifies the alternative exon sequence. The algorithm then extracts all possible sequences from the target sequence using a window of 20 nucleotides. Each 20mer is evaluated for valid GC content (between 30% and 80%), the absence of four consecutive identical nucleotides, and of immune stimulatory responses sequence motifs (39–42), and self-complementarity of the sequence ($\Delta G$ higher than −9.4 kcal/mol). Self-complementarity minimum energy folding was calculated using the hybrid-ss-min software included in the UNAFold package (38) using default parameters. The $\Delta G$ threshold was determined by calculating the average and standard deviation of 10 000 randomly generated 20mer sequences located at the 5′ end of TOSS. The threshold was fixed as the average plus two standard deviations to ensure that no strong intramolecular folding structure (lower than −9.4 kcal/mol) was formed. **(B)** Predictions that meet the above criteria's are then sorted according to different filters. First, each prediction is submitted to a Blast analysis (43) against an *in silico* generated transcriptome database derived from the Aceview annotation (44). This step is performed to determine potential

(continued)

interfered with RT-PCR in a manner quantitatively similar to TOSS (Supplementary Figure S5). Thus, the greater shifting activity of TOSS in cells cannot be explained by an artifactual impact on RT-PCR. Moreover, this increased efficiency in splicing modulation can directly be attributed to the recruitment of hnRNP A1 to the tail because mutations in the tail reduced the effect on splicing in all cases (Supplementary Table S1; Supplementary Figure S6).

In comparison to RNA or DNA, the 2′OMe composition of the tail remains the most efficient to promote exon skipping on the *KITLG* pre-mRNA (Supplementary Figure S7), as shown previously for modulation of 5′ss selection on *Bcl-x* (23). Although tails carrying a branched structure, a branch site or a 5′ss can provide repressor activity (23,24), we have used the hnRNP A1 tail for the remainder of the current TOSS analysis.

### Parameters of targets for optimal TOSS modulation

TOSS efficiency may be affected by the distance that separates its hybridization site from the target splice site. Indeed, *in vitro* studies on *Bcl-x* suggested that the impact of a TOSS decreased as the distance between its binding site and the targeted 5′ss increased (23). To determine if this observation applies to other pre-mRNAs *in vivo*, we tested TOSS harboring sequences complementary to various positions upstream of a 5′ss in two genes (*MCL1* and *SHMT1*). The results indicate that the distal positioning of TOSS (−31 and −38 on *MCL1*, and −49 and −58 on *SHMT1*) was the most efficient, and that a downstream exonic site either reduced TOSS efficiency or was as active (Figure 4). A TOSS targeting an intronic region downstream of an alternative 5′ss in *KITLG* had no impact (Supplementary Table S1). Although we have not identified the upstream limit for the impact of TOSS, efficient TOSS activity has so far been obtained by targeting the −1 to −60 region from the target 5′ss. The position that imposes maximal activity likely varies between targets most probably due to differences in secondary structure, the presence of regulatory elements and the existence of off-target hybridization sites that could reduce the effective concentration of TOSS.

To increase the utility of the different parameters influencing the modulation of alternative splicing we built a web interface-based program for TOSS design that takes into account structural and target features based from the above and our previous studies (23,24,32) (Figure 2; http://toss.lgfus.ca). We use the program to design TOSS targeting more complex pre-mRNAs. *NUP98* carries three competing 5′ss (Figure 5A) and we used two TOSS complementary to a region upstream of the more downstream 5′ss (Figure 5A). Using endpoint RT-PCR (Figure 5B), we monitored the level of inclusion of the long variant (Figure 5C). NUP98–TOSS1 had little impact, whereas NUP98–TOSS2 decreased the production of the long variant more importantly than NUP98–ASO2 (Figure 5C). Quantitative RT-PCR confirmed that the level of the short splice variant was strongly and specifically increased by NUP98–TOSS2 (Figure 5D).

To determine whether a TOSS could affect the splicing of an exon flanked by adjacent alternative exons, we targeted three double cassette exons units (*APP*, *FGFR2* and *FANCA*) and three units with triple adjacent alternative exons (*PTPN13*, *NRG1* and *BCAS1*). For each event, a TOSS was designed to target the first or the last alternative exon. Quantitative and endpoint RT-PCR were used to evaluate exon-specific and multiple exon splicing. Exon-specific modulation was noted in five of six cases (*APP*, *FGFR2*, *FANCA*, *PTPN13* and *BCAS1*; Supplementary Figure S8–S13), and a reduction in global expression was also observed in one case (*BCAS1*; Supplementary Figure S13). Overall, the TOSS remained specific to the targeted exon as the impact of TOSS on the splicing of non-targeted adjacent alternative exon was never observed.

In conclusion, we have tested a total of 89 TOSS and control oligonucleotides. The 'winner' designs proposed by the TOSS algorithm were active in 80% of the cases (24 of 30), as judged by endpoint RT-PCR (Supplementary Table S1). When Trizol extraction was not used for purifying RNA, quantitative RT-PCR confirmed that 17 of the 20 TOSS-mediated shifts were not artifacts caused by the presence of TOSS in the endpoint PCR mixtures. Although we have focused our study on the ability of TOSS to target 5′ss, modulating alternative 3′ss usage was attempted once with success (Supplementary Figure S14). Notably, some ASO and TOSS promoted global reduction in expression but the reasons for these effects are unclear. Thus, our study demonstrates that TOSS provides a robust approach that can promote dramatic shifts in the ratio of splice variants with limited impact on global expression levels.

### Development of a TOES that promotes exon inclusion

The antisense technology currently applied to splicing control mostly aims at preventing the binding of splicing factors. However, in some instances it may be useful to improve splice site recognition. One technology that has been developed to stimulate exon inclusion has been

**Figure 2.** Continued
off-targets associated with the hybridizing portion of the TOSS. Second, the sequence complementary to the hybridizing portion of the TOSS is evaluated for the potential presence of splicing enhancer (ESE) and splicing silencer (ESS) motif sequences. To perform this step, each nucleotide found in the input sequence was scored against a database of potential ESE and ESS motifs previously identified by Stadler *et al.* (45). If the nucleotide is part of an ESE or an ESS motif, the nucleotide score is increased or decreased by 1, respectively. The TOSS prediction is then attributed a global ESE/ESS score representing the sum of the nucleotides. Then, valid predictions are separated in two pools based on 5′ss distances; the first and second pool being, respectively, below and above a distance of 30 nucleotides from the 5′ splice junction. Once all filters are computed, both pools are then ordered to favor predictions with the least potential off-targets and the highest global ESE/ESS score to maximize disruption of potential enhancers. Finally, predictions from the pool closest to the 5′ss (<30 nucleotides) are favored over the long distance pool. The program web application can be accessed at http://toss.lgfus.ca.

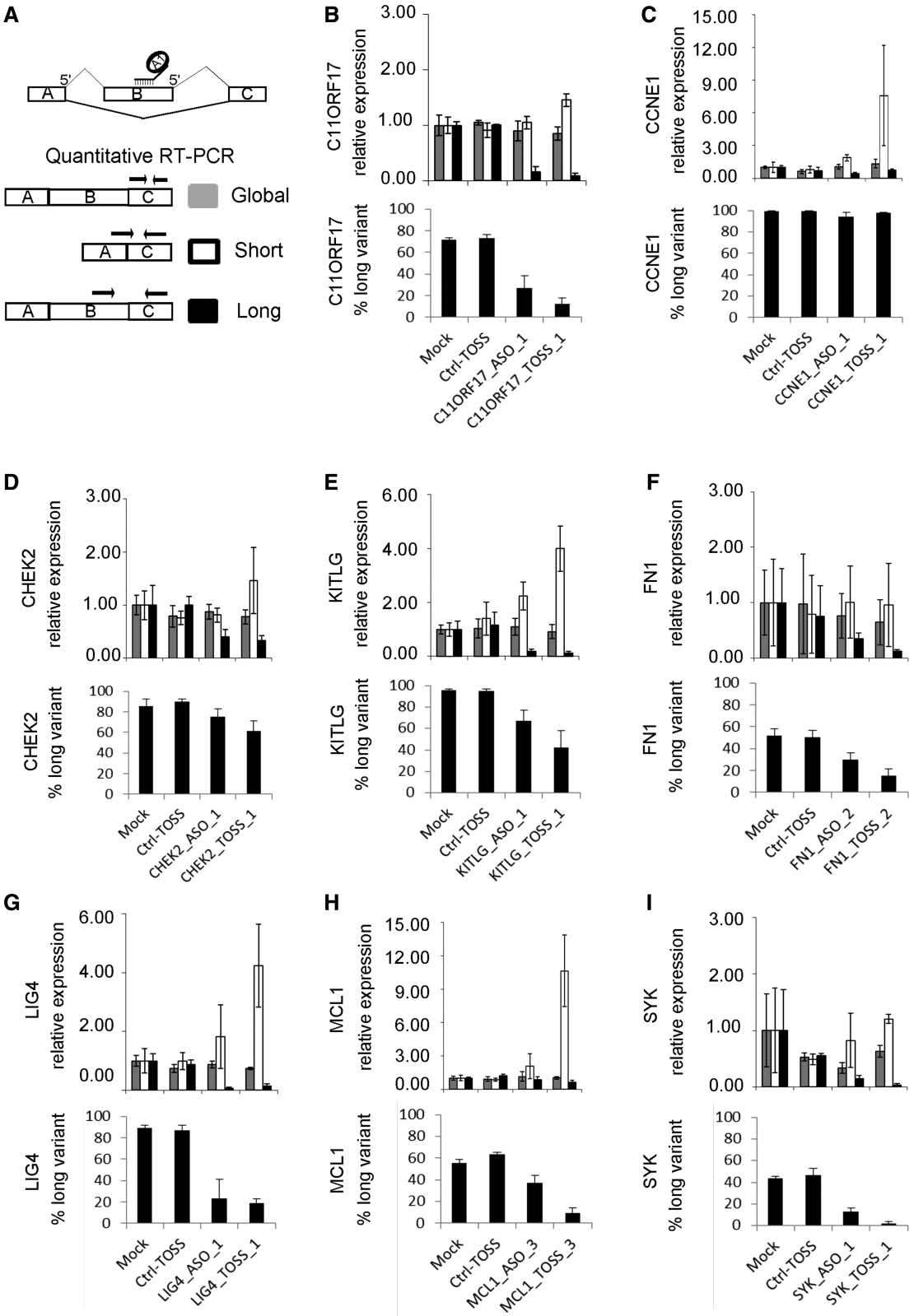


**Figure 3.** Effect of TOSS versus ASO. **(A)** Schematic representation of a standard cassette exon. The positions of qRT-PCR primers are indicated. **(B–I)** SKOV3ip1 cells were transfected with specific TOSS, their ASO versions (lacking a tail) and a control TOSS carrying no complementarity to the targeted gene. Total RNA was extracted 24 h later using *Absolutely RNA 96 Microprep kit* (Stratagene). Histograms represent average relative values for global expression (dark gray), short isoform (white) and the long isoform (black) obtained by quantitative RT-PCR in three biological replicates (upper portion of each panel). The quantitative RT-PCR values for the short and long isoforms were output as percentage of long variant for each condition (lower portion of each panel) using calculations described previously (32).

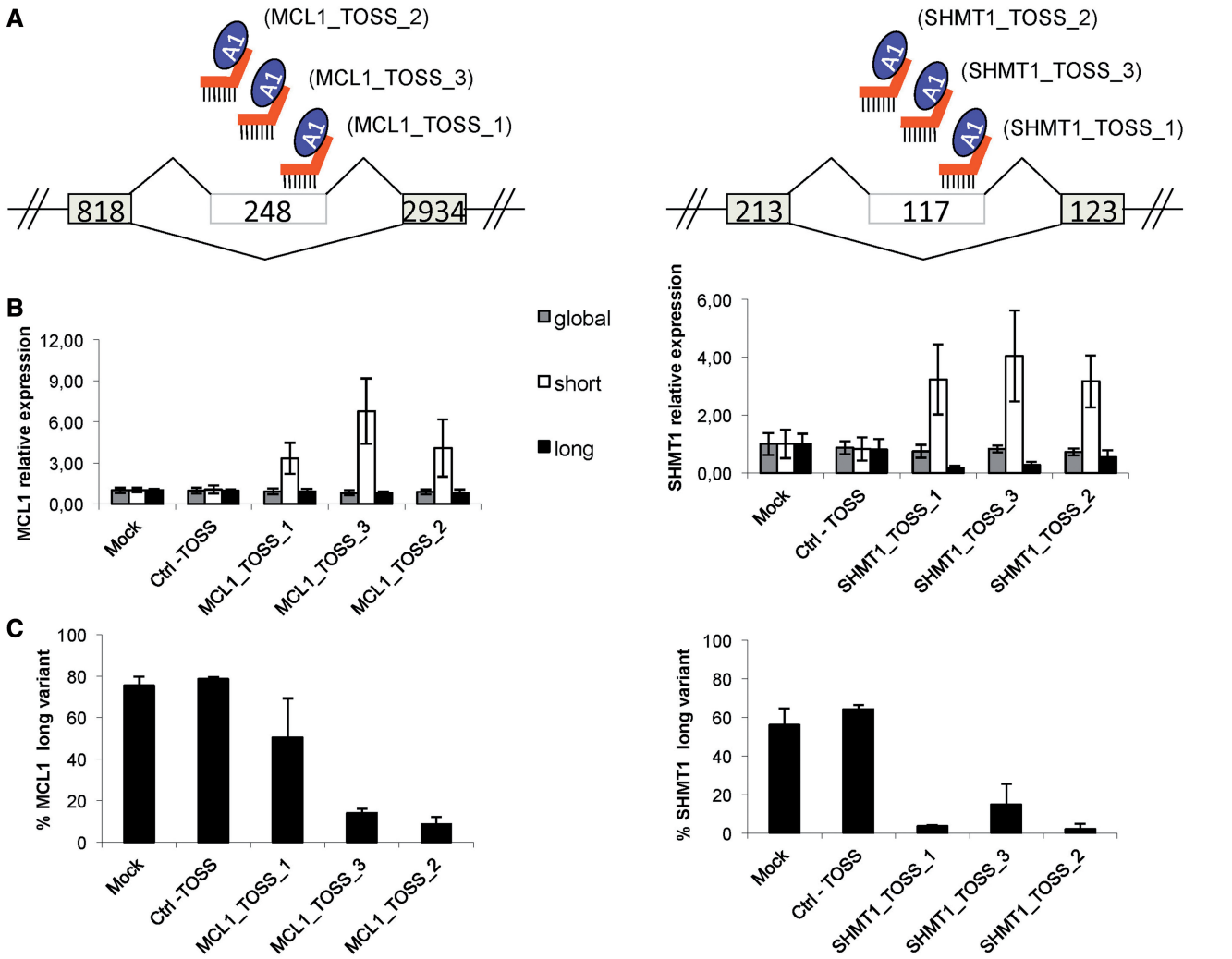


**Figure 4.** Impact of the distance relative to 5′ss on TOSS activity. **(A)** Schematic representation of *MCL1* (left panel) and *SHMT1* (right panel) cassette exon and the relative positions of TOSS to 5′ss. **(B)** SKOV3ip1 cells were transfected with TOSS harboring sequences complementary to various positions upstream of a 5′ss of the two genes (*MCL1* and *SHMT1*) and a control TOSS carrying no complementarity to the targeted genes (MCL1_TOSS_2 position −38; MCL1_TOSS_3 position −31; MCL1_TOSS_1 position −2; SHMT1_TOSS_2 position −58; SHMT1_TOSS_3 position −49 and SHMT1_TOSS_1 position 0). Total RNA was extracted 24 h later using *Absolutely RNA 96 Microprep kit* (Stratagene). Histograms represent average relative values for global expression (dark gray), short isoform (white) and the long isoform (black) obtained by quantitative RT-PCR in three biological replicates (upper panel). **(C)** Histograms represent average percentage values obtained by end-point PCR in three biological replicates.

bifunctional oligonucleotides that can recruit SR proteins (28). We tested a TOES design that uses a phosphorothioate SRSF1 binding tail (28). Alternative units in *LGALS9* and *KITLG* were targeted with SRSF1-recruiting TOES, and splicing was monitored using PCR. As expected, the TOES promoted exon inclusion in both cases (Supplementary Figure S15). However, we found that the phosphorothioate tail required for TOES activity was toxic for our ovarian and breast cancer cell lines, which makes these TOES difficult to use in functional assays. To avoid the toxic effects, we replaced the phosphorothioate tail with a 2′OMe tail, which has worked well for splicing repression using hnRNP A1. Unfortunately, TOES with 2′OMe tails failed to stimulate splicing presumably due to the lack of binding of SRSF1 (Supplementary Figure S15). We conclude that phosphorothioate TOES or 2′OMe TOES using SRSF1 are not practical for analyzing the impact of alternative splicing on cell functions.

To design TOES capable of modulating splicing without affecting cell viability we focused on TDP-43. This RNA-binding protein and splicing factor can bind with similar affinity to single-stranded TG and UG repeats (46), suggesting that its binding may tolerate 2′OMe nucleotide modifications. Its relatively high abundance also decreases the possibility that its partial sequestration by nanomolar quantities of TOES will impact normal TDP-43-mediated functions. The enhancing capacity of TDP-43 was tested by inserting the TDP-43 binding element (TBS) $(UG)_{13}$ downstream of a 5′ss in the model Dup 5.1 minigene which contains duplicated β-globin exon and intron sequences (Figure 6A). Since

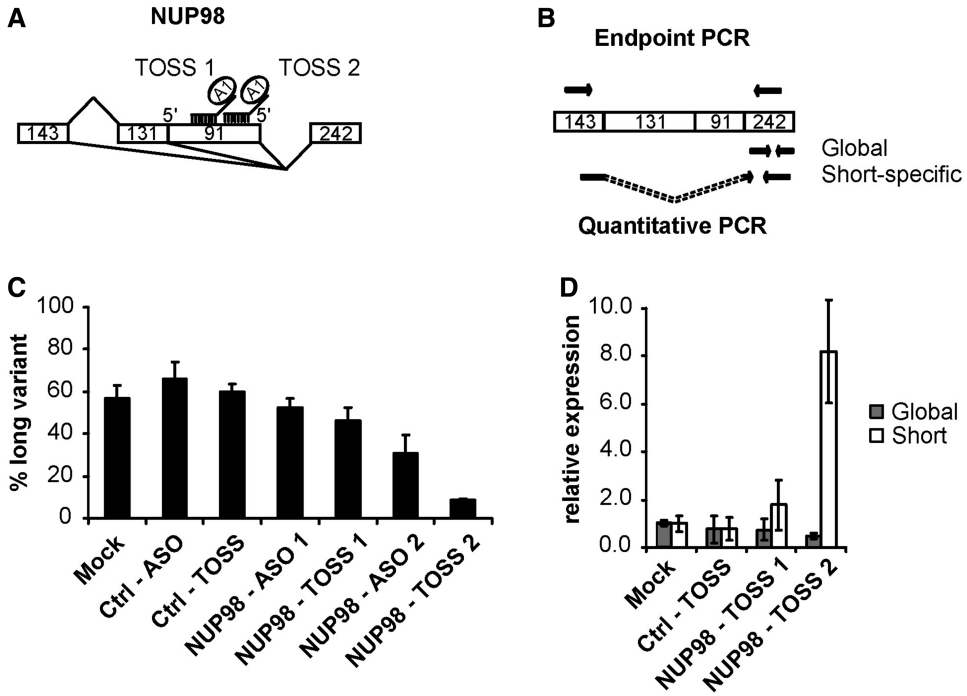


**Figure 5.** Using TOSS to redirect splicing in a complex unit carrying alternative 5′ss. **(A)** Schematic representation of the *NUP98* alternative splicing unit as well as the position of NUP98–TOSS1 and NUP98–TOSS2 on the 222 nt exon. **(B)** Positions of primers used to amplify splice variants of *NUP98* in endpoint and quantitative PCR assays. **(C)** SKOV3ip1 cells were transfected with NUP98–TOSS1, NUP98–TOSS2, their ASO versions (lacking a tail), and a control TOSS and ASO carrying no complementarity to *NUP98* (ctrl–TOSS and ctrl–ASO, respectively). Total RNA was extracted with Trizol 24 h later. Histograms representing average percentage values of the long variant obtained by endpoint PCR in three biological replicates are depicted. **(D)** SKOV3ip1 cells were transfected with NUP98–TOSS1, NUP98–TOSS2 and a control TOSS carrying an antisense sequence not complementary to *NUP98* (ctrl–TOSS). Total RNA was extracted 24 h later using the *Absolutely RNA 96 Microprep kit* (Stratagene). Histograms represent average relative values for global expression (dark gray) and the short (white) splice variant obtained by quantitative RT-PCR in three biological replicates.

skipping of the central exon was stimulated, the TBS appeared to improve selection of the 5′ss of the first exon relative to that of the central alternative exon (Figure 6B). This splicing shift was abrogated when cells were depleted of TDP-43 through expression of a shRNA (Figure 6B and C). It is possible that exon skipping in Dup 5.1 is caused by repression of the internal exon. To address the mechanism by which TDP-43 controls splice site selection we tested the impact of inserting UG repeats in model pre-mRNAs carrying a single intron. In the two different model pre-mRNAs tested, the presence of UG repeats positioned downstream from the 5′ss stimulated splicing in HeLa nuclear extracts (Supplementary Figure S16), indicating that intronic TDP-43 binding sites stimulate the use of the upstream 5′ss.

Next, we tested the TBS in a different model pre-mRNA (553) carrying two competing 5′ss (Figure 7A) as a prelude to measuring the impact of the TBS on U1 snRNP binding. Pre-mRNA splicing in a HeLa nuclear extract indicated that the TBS shifted splicing to favor the 5′ss directly upstream from the TBS (Figure 7B). We used this pre-mRNA to analyze U1 snRNP binding to the competing 5′ss through an oligonucleotide/RNAse H protection assay (35) and observed that the TBS improved U1 snRNP binding to the 5′ss directly upstream from it (Figure 7C and D).

Finally, we designed $(UG)_{10}$-carrying TOES targeting the disease-related human *SMN2* gene (Figure 8A). Improving the inclusion of alternative exon 7 in *SMN2* is used as a strategy to increase the production of the SMN protein in SMA patients who have lost the *SMN1* gene (13,14,19). The antisense portion of the TOES was complementary to positions +21 to +35 downstream of the 5′ss of exon 7, a position previously shown to be ineffective when targeted by an ASO (14). TOES were transfected in the Sma77 cell line derived from a SMA patient. As shown in Figure 8B, inclusion of exon 7 remained unchanged when the complementary ASO was used (lane 2), consistent with previous observations (14). In contrast, the presence of the $(UG)_{10}$ tail at the 5′ end of the TOES oligo increased exon inclusion (lane 3); a larger increase was obtained by positioning the TDP-43 binding tail at the 3′ end of TOES, possibly because of closer proximity of the tail to the target splice site (lane 4). As expected, the higher level of the exon 7-containing *SMN2* splice variant improved production of the SMN2 protein (Figure 8C). Because SMA cells have limited growth potential and do not support well successive transfections, we have been unable to confirm that the splicing shift in SMA cells is caused by TDP-43. Thus, while we would argue that the activity of the *trans*-acting TBS is mediated by TDP-43 (as was the *cis*-acting TBS in HeLa cells), we cannot rule out

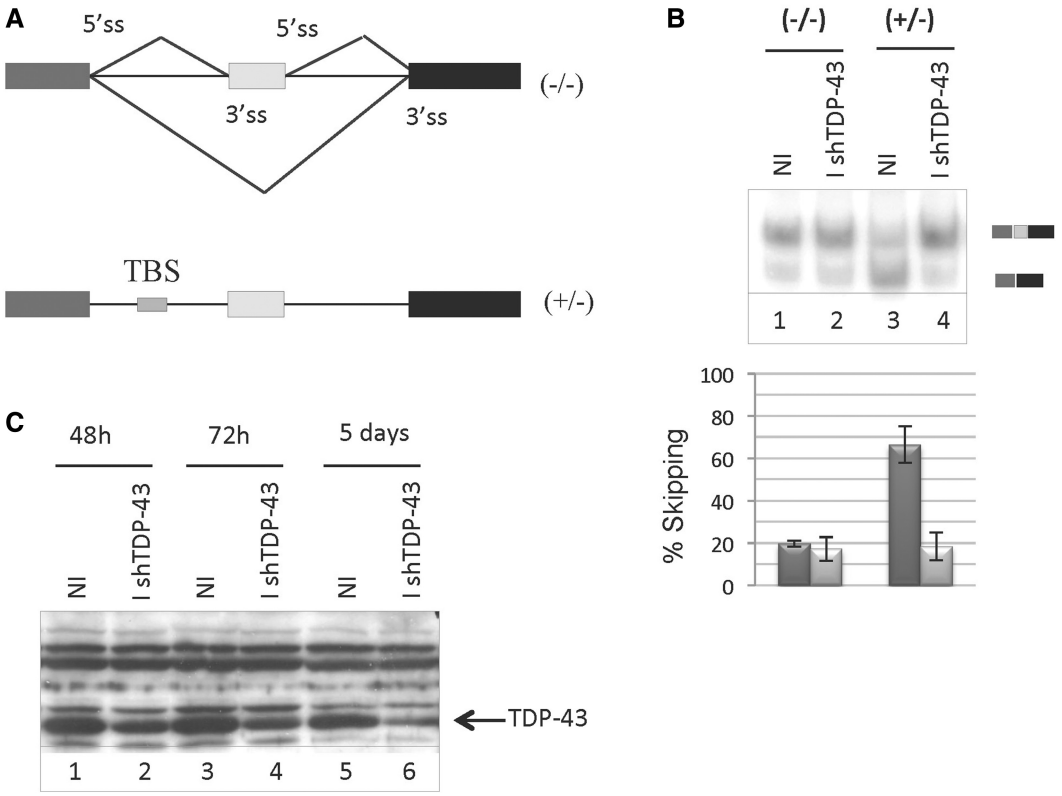


**Figure 6.** Impact of TDP-43 binding sites on splicing. **(A)** The Dup 5.1 minigene was used as model (47). The (−/−) is the wild-type version that contains an alternative cassette exon, while the (+/−) version contains a $(UG)_{13}$ element (TBS) in the first intron, 90 nt downstream from the 5′ss and 47 nt upstream of the 3′ss of the internal exon. **(B)** *In vivo* splicing of (−/−) and (+/−) in induced (I shTDP-43) and non-induced (NI) HeLa/shTDP-43 cells. Following an induction or mock-induction period of 48 h with doxycycline, plasmids were transfected and RNA collected 24 h later. RT-PCR products were fractionated on denaturing acrylamide gels, and the relative level of exon inclusion was calculated from biological triplicates. **(C)** Western analysis of TDP-43 expression in the induced (I shTDP-43) and NI HeLa/shTDP-43 cell line following doxycycline induction for the times indicated.

that other UG repeats binding proteins are contributing to the shift in SMA cells. The TOES containing a TDP-43 binding site, therefore, represents an interesting tool for improving the relative inclusion of *SMN2* exon 7. We conclude that TOES with TDP-43 binding sites are a practical alternative for improving exon inclusion, and for monitoring the impact of splicing shifts on cell functions since no apparent toxicity was noted following transfection.

## DISCUSSION

Alternative splicing is a powerful generator of protein diversity, and profiles of alternative splicing are often altered in human diseases, from muscular dystrophy to cancer. Procedures that can specifically decrease the level of splice variants or redirect splicing to favor the production of others can be useful to address the function of the continuously expanding repertoire of splice variants, and to correct or interfere with the production of splice isoforms in human maladies.

### TOSS

To generalize the use of bifunctional oligonucleotides as tools to modulate the production of splice variants, we have developed an algorithm that can design functional TOSS with a success rate of 80%. Using this program, we have successfully targeted 5′ss in genes displaying a variety of architecture including competing 5′ss as well as cassette exons in simple or more complex splicing units. By targeting a region upstream of an alternative 5′ss, there might be additional impact on gene expression since the hybridized TOSS or ASO may interfere with the deposition of the exon junction complex, possibly compromising mRNA transport and stability. Further interference may occur at the translational level. In all cases, however, altering these processes would contribute to the ultimate goal which is to repress specifically the expression of the splice variant. While most of the splicing shifts had minimal impact on the overall expression levels, some ASO and TOSS promoted decreases in global expression. The reasons for these effects are not understood but one possible mechanism may be chromatin-mediated, as shown for the Ago-mediated action of siRNAs (48).

Although we have not systematically investigated the ability of TOSS to modulate 3′ss choice, our single attempt at it was encouraging, suggesting that it should be possible to extract rules to achieve maximal interference on splicing units with different 3′ss configurations. All the TOSS that display repressing activity were

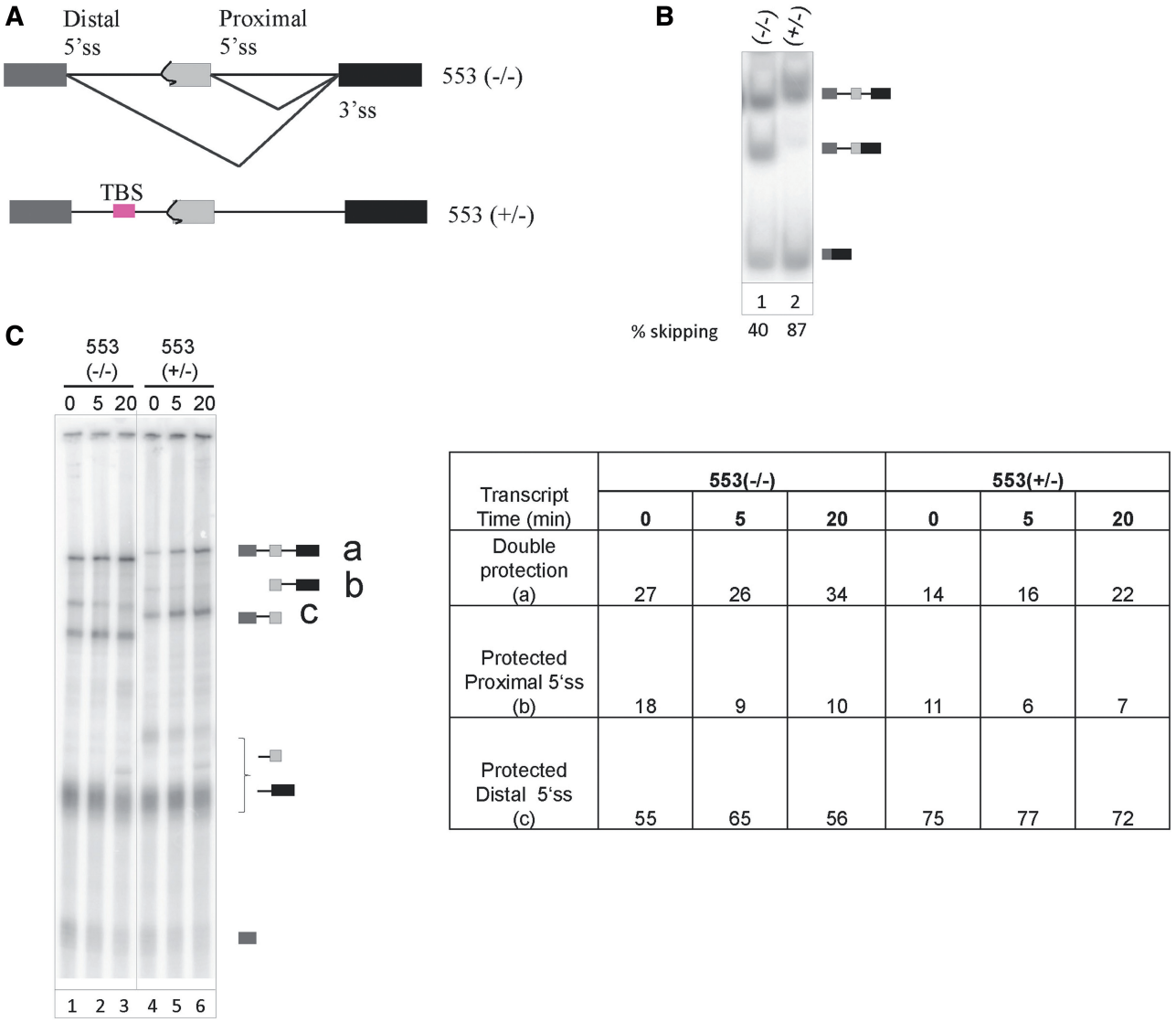


| Transcript Time (min) | 553(-/-) 0 | 553(-/-) 5 | 553(-/-) 20 | 553(+/-) 0 | 553(+/-) 5 | 553(+/-) 20 |
|---|---|---|---|---|---|---|
| Double protection (a) | 27 | 26 | 34 | 14 | 16 | 22 |
| Protected Proximal 5'ss (b) | 18 | 9 | 10 | 11 | 6 | 7 |
| Protected Distal 5'ss (c) | 55 | 65 | 56 | 75 | 77 | 72 |

**Figure 7.** TDP-43 stimulates U1 snRNP binding. **(A)** Structure of the model pre-mRNAs used to determine the *in vitro* impact of a binding site for TDP-43 [TBS made up of $(UG)_{13}$] on 5′ss selection. The 553 (−/−) pre-mRNA carries two competing 5′ss (distal and proximal). The 553 (+/−) pre-mRNA derivative carries a $(UG)_{13}$ TBS element 30 nt downstream of the distal 5′ss. **(B)** *In vitro* splicing of the two model pre-mRNAs for 90 min in a HeLa nuclear extract. The percentage of skipping of the proximal 5′ss is indicated. **(C)** Uniformly radiolabeled transcripts are incubated 0, 5 or 20 min at 30°C in a HeLa nuclear extract. Two DNA oligonucleotides complementary to each 5′ss are added along with RNase H which will cut the RNA moiety of the DNA:RNA duplex. Transcripts are therefore cut when U1 is not bound to the 5′ss. Cleavage products are separated on a denaturing acrylamide gel. The bands corresponding to double protection, proximal 5′ss protection only or distal 5′ss protection only are quantitated on PhosphorImager. The table indicates the normalized percentage of U1 snRNP occupancy at both 5′ss, at only the proximal 5′ss or only the distal 5′ss after incubation for 0, 5 and 20 min in a HeLa nuclear extract at 30°C.

complementary to the exonic region upstream of the targeted 5′ss (up to position −60 was tested). The tail portion of the TOSS was important in the majority of the cases, since a tail-less ASO was less likely to work or its impact was consistently lower than that of a TOSS. Although we have limited our current study to a tail bound by the hnRNP A1 protein, we have shown that tails of various architectures can repress splicing (24), suggesting that it should be possible to design repressing tails that recruit other RNA-binding proteins, provided that binding is not disrupted by the chemical modification used to improve the stability or delivery of the oligonucleotide.

Interestingly, bifunctional oligonucleotides with an hnRNP A1-bound tail can also be used to stimulate splicing when they are positioned downstream of a 5′ss (49). This activity has been associated with the presence of additional hnRNP A1 binding sites located further downstream in the intron, and we have proposed that stimulation occurs when an interaction between multiple bound hnRNP A1 approximate the ends of the intron to favor spliceosome assembly (49). A similar A1/A1 interaction across an exon may lead to repression (50,51), possibly explaining why intronic A1 binding elements can also be silencers (18). On the other hand, we have observed that recruiting hnRNP A1 downstream of the 5′ss in

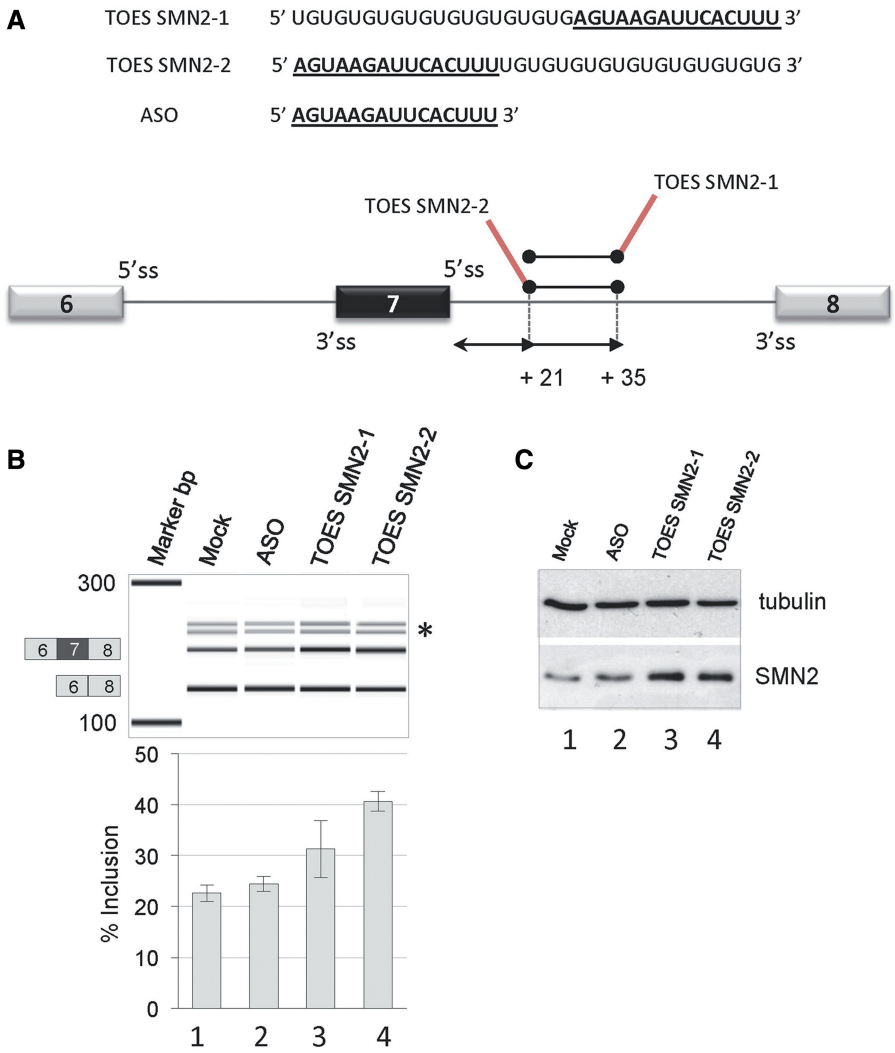


**Figure 8.** TOES-mediated exon inclusion on *SMN2* transcripts. **(A)** A portion of the *SMN2* gene was targeted with TDP-43-TOES complementary to positions +21 to +35 downstream of exon 7. The portion of the oligos complementary to *SMN2* is underlined. **(B)** RNA was extracted 48 h post-transfection. Computerized versions of electropherograms are shown as well as a histogram with standard deviations derived from biological triplicates. Primers used for *SMN2* amplification were 54C618 (sense) 5′-CTCCCATATGTCCAGATTCTCTT-3′ and 541C1120 (antisense) 5′-CTACAACACCCTTCTCACAG-3′. The position, structure and size of the amplification products corresponding to the splice variants are shown. The identity of the doublet bands (*) migrating above the two *SMN2* splice products is unknown. The graph displays the inclusion frequency (in percentage) of *SMN2* exon 7 based on biological triplicates. **(C)** Expression of the SMN2 protein was analyzed in one set by western blot 72 h after transfection with using anti-human SMN antibodies (BD Transduction Labs).

*KITLG* had no effect. Thus, the impact of an hnRNP A1 binding site located downstream of a 5′ss may vary according to the presence and position of additional high affinity sites for hnRNP A1 on the pre-mRNA.

## TOES

Considerably less attention has been devoted to oligonucleotides designed to stimulate splicing by recruiting or mimicking splicing regulators. Furthermore, we found that phosphorothioate oligonucleotides were cytotoxic and that 2′OMe versions designed to recruit the positive splicing factor SRSF1 were inactive most likely because they were incompatible with efficient protein binding. Possibly for the same reason, we have been unable to document the activity of 2′OMe tails with sequences normally recognized by RBFOX proteins (data not shown).

Because the above observations limited our ability to test TOES on a variety of targets, we instead aimed at identifying a protein that could stimulate 5′ss usage when positioned downstream from a 5′ss and that could act when recruited by a tailed 2′OMe oligonucleotide. We focused on TDP-43 because this hnRNP-like protein displays similarly strong binding to RNA and DNA (46), suggesting that it could also interact with a 2′OMe-modified sequence. While a role for TDP-43 in 3′ss control is well established (46), a function in 5′ss selection is more ambiguous (52). We first showed that *cis*-acting TDP-43 binding sites positioned downstream of a 5′ss could stimulate splicing in two different model genes; in one case the

stimulation correlating with increased U1 snRNP binding at the targeted 5′ss. The potential of TDP-43-binding tails was then validated by showing that TDP-43 binding sites in the tail of a bifunctional oligonucleotide complementary to a region downstream of *SMN2* exon 7 shifted splicing to favor exon inclusion.

In conclusion, our studies have increased the variety of tools that can be used alone or in combination with RNAi approaches to investigate the function of splice variants or to repress or improve the use of specific splice sites associated with a disease. TOSS or TOES carrying 2′OMe tails provide a practical approach that specifically redirect splicing with no apparent toxic impact, thereby keeping cells in a state where they can benefit from a newly acquired function or display information on a new phenotype imposed by the altered production of splice variants.

## SUPPLEMENTARY DATA

Supplementary Data are available at NAR Online.

## ACKNOWLEDGEMENTS

We thank Johanne Toutant and Sonia Couture for help with tissue culture and extract preparation. We thank Douglas Black for Dup 5.1, Jocelyn Côté for the SMA patient cell line, Emanuele Buratti and Francisco Baralle for the TDP-43 antibody and Andrés Aguilera for pTER+ and pCDNA 6/TR plasmids used to produce the inducible shRNA against TDP-43.

## FUNDING

This research project was supported by CIHR grants [MOP-272013 to S.A.E. and MOP-93791 to B.C.]; the Chaire de recherche de l'Université de Sherbrooke on RNA Structure and Genomics (to J.-P.P.); the Canada Research Chair in RNA Biology and Cancer Genomics (to S.A.E.); the Canada Research Chair in Functional Genomics (to B.C.); members of the Centre d'excellence de l'Université de Sherbrooke en biologie de l'ARN (to B.C., S.A.E and J.-P.P). Funding for open access charge: Canadian Institute for Health Research.

*Conflict of interest statement*. None declared.

## REFERENCES

1. Pan,Q., Shai,O., Lee,L.J., Frey,B.J. and Blencowe,B.J. (2008) Deep surveying of alternative splicing complexity in the human transcriptome by high-throughput sequencing. *Nat. Genet.*, **40**, 1413–1415.
2. Wang,E.T., Sandberg,R., Luo,S., Khrebtukova,I., Zhang,L., Mayr,C., Kingsmore,S.F., Schroth,G.P. and Burge,C.B. (2008) Alternative isoform regulation in human tissue transcriptomes. *Nature*, **456**, 470–476.
3. Djebali,S., Davis,C.A., Merkel,A., Dobin,A., Lassmann,T., Mortazavi,A., Tanzer,A., Lagarde,J., Lin,W., Schlesinger,F. *et al.* (2012) Landscape of transcription in human cells. *Nature*, **489**, 101–108.
4. Nilsen,T.W. and Graveley,B.R. (2010) Expansion of the eukaryotic proteome by alternative splicing. *Nature*, **463**, 457–463.
5. Tazi,J., Bakkour,N. and Stamm,S. (2009) Alternative splicing and disease. *Biochim. Biophys. Acta*, **1792**, 14–26.
6. Venables,J.P., Klinck,R., Koh,C., Gervais-Bird,J., Bramard,A., Inkel,L., Durand,M., Couture,S., Froehlich,U., Lapointe,E. *et al.* (2009) Cancer-associated regulation of alternative splicing. *Nat. Struct. Mol. Biol.*, **16**, 670–676.
7. Lopez-Bigas,N., Audit,B., Ouzounis,C., Parra,G. and Guigo,R. (2005) Are splicing mutations the most frequent cause of hereditary disease? *FEBS Lett.*, **579**, 1900–1903.
8. Park,J.W., Parisky,K., Celotto,A.M., Reenan,R.A. and Graveley,B.R. (2004) Identification of alternative splicing regulators by RNA interference in Drosophila. *Proc. Natl Acad. Sci. U.S.A.*, **101**, 15974–15979.
9. Dominski,Z. and Kole,R. (1993) Restoration of correct splicing in thalassemic pre-mRNA by antisense oligonucleotides. *Proc. Natl Acad. Sci. U.S.A.*, **90**, 8673–8677.
10. Zammarchi,F., de Stanchina,E., Bournazou,E., Supakorndej,T., Martires,K., Riedel,E., Corben,A.D., Bromberg,J.F. and Cartegni,L. (2011) Antitumorigenic potential of STAT3 alternative splicing modulation. *Proc. Natl Acad. Sci. U.S.A.*, **108**, 17779–17784.
11. Garcia-Blanco,M.A. (2006) Alternative splicing: therapeutic target and tool. *Prog. Mol. Subcell. Biol.*, **44**, 47–64.
12. Kole,R., Krainer,A.R. and Altman,S. (2012) RNA therapeutics: beyond RNA interference and antisense oligonucleotides. *Nat. Rev. Drug Discov.*, **11**, 125–140.
13. Singh,N.K., Singh,N.N., Androphy,E.J. and Singh,R.N. (2006) Splicing of a critical exon of human Survival Motor Neuron is regulated by a unique silencer element located in the last intron. *Mol. Cell. Biol.*, **26**, 1333–1346.
14. Hua,Y., Vickers,T.A., Baker,B.F., Bennett,C.F. and Krainer,A.R. (2007) Enhancement of SMN2 exon 7 inclusion by antisense oligonucleotides targeting the exon. *PLoS Biol.*, **5**, e73.
15. Gallagher,T.L., Arribere,J.A., Geurts,P.A., Exner,C.R., McDonald,K.L., Dill,K.K., Marr,H.L., Adkar,S.S., Garnett,A.T., Amacher,S.L. *et al.* (2011) Rbfox-regulated alternative splicing is critical for zebrafish cardiac and skeletal muscle functions. *Dev. Biol.*, **359**, 251–261.
16. Hua,Y., Sahashi,K., Hung,G., Rigo,F., Passini,M.A., Bennett,C.F. and Krainer,A.R. (2010) Antisense correction of SMN2 splicing in the CNS rescues necrosis in a type III SMA mouse model. *Genes Dev.*, **24**, 1634–1644.
17. Hua,Y., Sahashi,K., Rigo,F., Hung,G., Horev,G., Bennett,C.F. and Krainer,A.R. (2011) Peripheral SMN restoration is essential for long-term rescue of a severe spinal muscular atrophy mouse model. *Nature*, **478**, 123–126.
18. Hua,Y., Vickers,T.A., Okunola,H.L., Bennett,C.F. and Krainer,A.R. (2008) Antisense masking of an hnRNP A1/A2 intronic splicing silencer corrects SMN2 splicing in transgenic mice. *Am. J. Hum. Genet.*, **82**, 834–848.
19. Spitali,P. and Aartsma-Rus,A. (2012) Splice modulating therapies for human disease. *Cell*, **148**, 1085–1088.
20. Cirak,S., Feng,L., Anthony,K., Arechavala-Gomeza,V., Torelli,S., Sewry,C., Morgan,J.E. and Muntoni,F. (2012) Restoration of the dystrophin-associated glycoprotein complex after exon skipping therapy in Duchenne muscular dystrophy. *Mol. Ther.*, **20**, 462–467.
21. Lu,Q.L., Rabinowitz,A., Chen,Y.C., Yokota,T., Yin,H., Alter,J., Jadoon,A., Bou-Gharios,G. and Partridge,T. (2005) Systemic delivery of antisense oligoribonucleotide restores dystrophin expression in body-wide skeletal muscles. *Proc. Natl Acad. Sci. U.S.A.*, **102**, 198–203.
22. Wu,B., Moulton,H.M., Iversen,P.L., Jiang,J., Li,J., Li,J., Spurney,C.F., Sali,A., Guerron,A.D., Nagaraju,K. *et al.* (2008) Effective rescue of dystrophin improves cardiac function in dystrophin-deficient mice by a modified morpholino oligomer. *Proc. Natl Acad. Sci. U.S.A.*, **105**, 14814–14819.
23. Villemaire,J., Dion,I., Elela,S.A. and Chabot,B. (2003) Reprogramming alternative pre-messenger RNA splicing through the use of protein-binding antisense oligonucleotides. *J. Biol. Chem.*, **278**, 50031–50039.

24. Gendron,D., Carriero,S., Garneau,D., Villemaire,J., Klinck,R., Elela,S.A., Damha,M.J. and Chabot,B. (2006) Modulation of 5′ splice site selection using tailed oligonucleotides carrying splicing signals. *BMC Biotechnol.*, **6**, 5.
25. Dickson,A., Osman,E. and Lorson,C.L. (2008) A negatively acting bifunctional RNA increases survival motor neuron both in vitro and in vivo. *Hum. Gene Ther.*, **19**, 1307–1315.
26. Martinez-Contreras,R., Cloutier,P., Shkreta,L., Fisette,J.F., Revil,T. and Chabot,B. (2007) hnRNP proteins and splicing control. *Adv. Exp. Med. Biol.*, **623**, 123–147.
27. Garcia-Blanco,M.A., Baraniak,A.P. and Lasda,E.L. (2004) Alternative splicing in disease and therapy. *Nat. Biotechnol.*, **22**, 535–546.
28. Skordis,L.A., Dunckley,M.G., Yue,B., Eperon,I.C. and Muntoni,F. (2003) Bifunctional antisense oligonucleotides provide a trans-acting splicing enhancer that stimulates SMN2 gene expression in patient fibroblasts. *Proc. Natl Acad. Sci. U.S.A.*, **100**, 4114–4119.
29. Cartegni,L. and Krainer,A.R. (2003) Correction of disease-associated exon skipping by synthetic exon-specific activators. *Nat. Struct. Biol.*, **10**, 120–125.
30. Marquis,J., Meyer,K., Angehrn,L., Kampfer,S.S., Rothen-Rutishauser,B. and Schumperli,D. (2007) Spinal muscular atrophy: SMN2 pre-mRNA splicing corrected by a U7 snRNA derivative carrying a splicing enhancer sequence. *Mol. Ther.*, **15**, 1479–1486.
31. Venables,J.P., Brosseau,J.P., Gadea,G., Klinck,R., Prinos,P., Beaulieu,J.F., Lapointe,E., Durand,M., Thibault,P., Tremblay,K. *et al.* (2013) RBFOX2 is an important regulator of mesenchymal tissue-specific splicing in both normal and cancer tissues. *Mol. Cell. Biol.*, **33**, 396–405.
32. Prinos,P., Garneau,D., Lucier,J.F., Gendron,D., Couture,S., Boivin,M., Brosseau,J.P., Lapointe,E., Thibault,P., Durand,M. *et al.* (2011) Alternative splicing of SYK regulates mitosis and cell survival. *Nat. Struct. Mol. Biol.*, **18**, 673–679.
33. Brosseau,J.P., Lucier,J.F., Lapointe,E., Durand,M., Gendron,D., Gervais-Bird,J., Tremblay,K., Perreault,J.P. and Elela,S.A. (2010) High-throughput quantification of splicing isoforms. *RNA*, **16**, 442–449.
34. Klinck,R., Bramard,A., Inkel,L., Dufresne-Martin,G., Gervais-Bird,J., Madden,R., Paquet,E.R., Koh,C., Venables,J.P., Prinos,P. *et al.* (2008) Multiple alternative splicing markers for ovarian cancer. *Cancer Res.*, **68**, 657–663.
35. Chabot,B., Blanchette,M., Lapierre,I. and La Branche,H. (1997) An intron element modulating 5′ splice site selection in the hnRNP A1 pre-mRNA interacts with hnRNP A1. *Mol. Cell. Biol.*, **17**, 1776–1786.
36. Dignam,J.D., Lebovitz,R.M. and Roeder,R.G. (1983) Accurate transcription initiation by RNA polymerase II in a soluble extract from isolated mammalian nuclei. *Nucleic Acids Res.*, **11**, 1475–1489.
37. Brosseau,J.-P. (2012) *Ph.D. Thesis*, Université de Sherbrooke, Détection, annotation fonctionnelle et régulation des isoformes de l'épissage alternatif associées au cancer de l'ovaire.
38. Markham,N.R. and Zuker,M. (2008) UNAFold: software for nucleic acid folding and hybridization. *Methods Mol. Biol.*, **453**, 3–31.
39. Hornung,V., Guenthner-Biller,M., Bourquin,C., Ablasser,A., Schlee,M., Uematsu,S., Noronha,A., Manoharan,M., Akira,S., de Fougerolles,A. *et al.* (2005) Sequence-specific potent induction of IFN-alpha by short interfering RNA in plasmacytoid dendritic cells through TLR7. *Nat. Med.*, **11**, 263–270.
40. Judge,A.D., Sood,V., Shaw,J.R., Fang,D., McClintock,K. and MacLachlan,I. (2005) Sequence-dependent stimulation of the mammalian innate immune response by synthetic siRNA. *Nat. Biotechnol.*, **23**, 457–462.
41. Fedorov,Y., Anderson,E.M., Birmingham,A., Reynolds,A., Karpilow,J., Robinson,K., Leake,D., Marshall,W.S. and Khvorova,A. (2006) Off-target effects by siRNA can induce toxic phenotype. *RNA*, **12**, 1188–1196.
42. Pei,Y. and Tuschl,T. (2006) On the art of identifying effective and specific siRNAs. *Nat. Methods*, **3**, 670–676.
43. Altschul,S.F., Gish,W., Miller,W., Myers,E.W. and Lipman,D.J. (1990) Basic local alignment search tool. *J. Mol. Biol.*, **215**, 403–410.
44. Thierry-Mieg,D. and Thierry-Mieg,J. (2006) AceView: a comprehensive cDNA-supported gene and transcripts annotation. *Genome Biol.*, **7(Suppl. 1)**, S12.11–14.
45. Stadler,M.B., Shomron,N., Yeo,G.W., Schneider,A., Xiao,X. and Burge,C.B. (2006) Inference of splicing regulatory activities by sequence neighborhood analysis. *PLoS Genet.*, **2**, e191.
46. Buratti,E. and Baralle,F.E. (2001) Characterization and functional implications of the RNA binding properties of nuclear factor TDP-43, a novel splicing regulator of CFTR exon 9. *J. Biol. Chem.*, **276**, 36337–36343.
47. Simard,M.J. and Chabot,B. (2000) Control of hnRNP A1 alternative splicing: an intron element represses use of the common 3′ splice site. *Mol. Cell. Biol.*, **20**, 7353–7362.
48. Allo,M., Buggiano,V., Fededa,J.P., Petrillo,E., Schor,I., de la Mata,M., Agirre,E., Plass,M., Eyras,E., Elela,S.A. *et al.* (2009) Control of alternative splicing through siRNA-mediated transcriptional gene silencing. *Nat. Struct. Mol. Biol.*, **16**, 717–724.
49. Martinez-Contreras,R., Fisette,J.F., Nasim,F.U., Madden,R., Cordeau,M. and Chabot,B. (2006) Intronic binding sites for hnRNP A/B and hnRNP F/H proteins stimulate pre-mRNA splicing. *PLoS Biol.*, **4**, e21.
50. Nasim,F.U., Hutchison,S., Cordeau,M. and Chabot,B. (2002) High-affinity hnRNP A1 binding sites and duplex-forming inverted repeats have similar effects on 5′ splice site selection in support of a common looping out and repression mechanism. *RNA*, **8**, 1078–1089.
51. Blanchette,M. and Chabot,B. (1999) Modulation of exon skipping by high-affinity hnRNP A1-binding sites and by intron elements that repress splice site utilization. *EMBO J.*, **18**, 1939–1952.
52. Passoni,M., De Conti,L., Baralle,M. and Buratti,E. (2012) UG repeats/TDP-43 interactions near 5′ splice sites exert unpredictable effects on splicing modulation. *J. Mol. Biol.*, **415**, 46–60.